POLITECNICO DI TORINO
Repository ISTITUZIONALE

Mitigating vector-borne diseases on networks: A feasible and stable nonlinear MPC approach

Original
Mitigating vector-borne diseases on networks: A feasible and stable nonlinear MPC approach / Raineri, R., Pagone, M., Zino, L., Rizzo, A.. - In: NONLINEAR ANALYSIS. - ISSN 1751-570X. - STAMPA. - 61:(2026). [10.1016/j.nahs.2026.101719]

Availability:
This version is available at: 11583/3009483 since: 2026-04-01T01:50:14Z

Publisher:
Elsevier

Published
DOI:10.1016/j.nahs.2026.101719

Terms of use:

This article is made available under terms and conditions as specified in the corresponding bibliographic description in the repository

Publisher copyright

(Article begins on next page)

19 November 2026

Nonlinear Analysis: Hybrid Systems 61 (2026) 101719

Contents lists available at ScienceDirect

Nonlinear Analysis: Hybrid Systems

journal homepage: www.elsevier.com/locate/nahs

Mitigating vector-borne diseases on networks: A feasible and stable nonlinear MPC approach☆,☆☆

Roberta Raineri, Michele Pagone *, Lorenzo Zino, Alessandro Rizzo

Department of Electronics and Telecommunications, Politecnico di Torino, 10129 Torino, Italy

ARTICLE INFO

Keywords:
Control over networks
Control of networks
Model predictive control
Complex dynamic systems
Interconnected nonlinear systems
Dynamics and control of biologically motivated nonlinear systems

ABSTRACT

In this paper, we deal with the problem of controlling a vector-borne epidemic disease, evolving over a network. In particular, we consider a discrete-time implementation of a network epidemic model consisting of two interacting populations of humans and vectors in each node of the network. In our model, humans can travel and become infected upon interaction with carrier vectors, while vectors can become carriers if interacting with infected humans. We devise an optimal control strategy by incorporating two control actions, associated with (i) human mobility restriction across the network, and (ii) reduction of carrier population. The control problem is solved by leveraging a nonlinear model predictive control for which we guarantee both the closed-loop stability and the recursive feasibility through a suitable selection of the terminal ingredients. The latter are determined by solving, offline, a dual optimization problem. Finally, we demonstrate our approach on a case study calibrated on realistic data.

1. Introduction

Recent advances in the mathematical modeling of epidemic diseases have facilitated the application of control-theoretic methods to design and evaluate interventions aimed at controlling their spread [1–4]. However, these models are predominantly constructed to address human-to-human transmission mechanisms [1,2,5,6]. On the one hand, this makes them suitable for describing several diseases, such as airborne infections and sexually transmitted illnesses. On the other hand, numerous serious diseases (e.g., dengue, malaria, and West Nile fever) are transmitted by arthropod vectors, such as mosquitoes and ticks, which can harbor pathogens and subsequently transmit them to humans [7]. Models based solely on human-to-human transmission cannot capture the vector-to-human and human-to-vector dynamics that characterize vector-borne diseases, making them unsuitable for guiding interventions targeting these infections.

To fill in this gap, numerous mathematical models for vector-borne diseases have been proposed and studied [8,9]. However, this body of literature has focused primarily on providing simulation tools that, while accurate, are often too complex to facilitate the application of control-theoretic tools in designing effective intervention policies. In fact, the vast majority of model-based studies on vector-borne disease control rely on an extensive campaign of numerical simulations, but lack theoretical guarantees [8,9].

☆ This article is part of a Special issue entitled: 'TC 1.5 Networked systems (IFAC WC 2026)' published in Nonlinear Analysis: Hybrid Systems.

☆☆ This study was carried out within the 2022K8EZBW "Higher-order interactions in social dynamics with application to monetary networks" project — funded by European Union — Next Generation EU within the PRIN 2022 program (D.D. 104 — 02/02/2022 Ministero dell'Università e della Ricerca). This manuscript reflects only the authors' views and opinions and the Ministry cannot be considered responsible for them.

* Corresponding author.

E-mail addresses: roberta.raineri@polito.it (R. Raineri), michele.pagone@polito.it (M. Pagone), lorenzo.zino@polito.it (L. Zino), alessandro.rizzo@polito.it (A. Rizzo).

https://doi.org/10.1016/j.nahs.2026.101719
Received 31 October 2025; Received in revised form 23 January 2026; Accepted 30 March 2026

Available online 31 March 2026
1751-570X/© 2026 The Authors. Published by Elsevier Ltd. This is an open access article under the CC BY license (http://creativecommons.org/licenses/by/4.0/).

To address this limitation, substantial effort has been devoted to developing parsimonious models for vector-borne diseases that effectively balance accuracy with tractability. For example, Zino et al. [10] proposed a model that is based on a classical continuous-time susceptible–infected–susceptible (SIS) framework [5], with interacting populations of humans and vectors. Humans can become infected through interactions with carrier vectors, vectors can become carriers after interacting with infected humans. Similar models were proposed in [11,12]. Building on these models, some control actions were studied, such as in [11], where time-invariant control policies were designed; or in [12–14], where optimal (time-varying) control policies were developed using Pontryagin's Maximum Principle. However, these approaches typically assume constant policies [11] or a fully-mixed population [12–14], limiting the possibility of exploring effective dynamic and targeted intervention policies, leveraging the heterogeneity of human and vector geographic distribution.

In this study, we extend the model presented in [10] to devise intervention strategies to mitigate the outbreak of a vector-borne disease. Specifically, after embedding the model from Zino et al. [10] (referred to hereafter as *human-vector-SIS* or HV-SIS) into a geographical network framework and establishing some fundamental insights into the well-posedness and equilibria of the uncontrolled dynamics, we introduce two control measures into the epidemic model. These measures involve: (i) limiting human mobility to areas where the disease is prevalent; and (ii) reducing the vector population through methods such as insecticide application or integrated pest management. Our primary research objective is to determine how to effectively combine these two intervention strategies in a cost-effective manner to curb the spread of vector-borne diseases while minimizing the costs associated with implementing the interventions.

In this context, model predictive control (MPC) has emerged as a potent tool in addressing complex dynamics and nonlinear multi-variable systems, including those arising from networks [15,16]. Its efficacy is due to its intrinsic capability to explicitly manage nonlinear dynamics and deliver optimal control commands for multi-variable systems, even amidst input, output, and state constraints [17]. Consequently, the applications of MPC have expanded beyond the conventional engineering and industrial spheres. In particular, in recent years, the COVID-19 pandemic has prompted the automatic control community to leverage MPC to guide policymakers to mitigate the spread of the epidemic, balancing health and socioeconomic outcomes [16,18–21]. However, these approaches are based on mathematical models that assume human-to-human transmission, which limits their applicability to vector-borne diseases, as they do not explicitly capture the joint spread of infection across two distinct species or the nonlinear nature of cross-species transmission mechanisms.

Motivated by these reasons, in this paper we propose a nonlinear Model Predictive Control (NMPC) approach for managing a vector-borne epidemic disease spreading on a network. Specifically, we devise a centralized control system designed to emulate policymakers in formulating mitigation strategies. The use of a centralized controller is justified by the organizational structure of healthcare systems, which are typically governed by a central decision-maker responsible for implementing policies that may vary across different locations. The NMPC is tasked with steering the system towards a desired equilibrium state for the HV-SIS dynamics, based on policymaker decisions.

Despite the success of MPC approaches in many fields of application, it is important to mention that ensuring closed-loop stability and recursive feasibility within an NMPC framework remains a challenging endeavor. In fact, these properties often depend on the appropriate selection of the terminal ingredients, namely, a terminal cost (e.g., a control Lyapunov function), a terminal constraint set (which is control admissible and invariant), and a terminal local stabilizing control law. Unlike the linear scenario, where the quasi-infinite horizon MPC scheme (see, e.g., Chen and Allgöwer [22]) provides straightforward guidelines for constructing the terminal ingredients, in the nonlinear context there are no closed-form solutions for the cost-to-go or the terminal control law. Both stability and constraint satisfaction can only be verified locally, thereby significantly increasing the design complexity. This challenge has been addressed over the past few decades [23–25]. A commonly adopted approach involves using a local linearization of the nonlinear dynamics around the equilibrium to be regulated. Simple solutions to the problem include imposing a terminal equality constraint with no terminal cost or omitting terminal ingredients, at the cost of a significant reduction in the domain of attraction of the controller [24]. Other similar strategies propose a linear-time variant modeling technique and a partition method to determine both the terminal cost and the terminal set [26,27]. These latter are more laborious to apply, but results in reduced conservativeness of the volume of the terminal set enlarging, then, the controller domain of attraction.

In this paper, we provide closed-loop stability and recursive feasibility of the NMPC framework by using a first-order Taylor approximation of the system dynamics to design terminal ingredients through the offline solution of a set of linear matrix inequalities (LMIs), as outlined in [28]. Furthermore, an offline nonlinear optimization problem is solved to validate the terminal ingredients of the nonlinear system previously determined. The proposed methodology provides an efficient and theoretically rigorous procedure to ensure recursive feasibility and closed-loop stability for the proposed NMPC formulation applied to epidemic network dynamics. Compared to Wan and Kothare [26,27], the approach employed here provides a more favorable balance between ease of implementation and conservativeness in the definition of the terminal set volume. Note that, as suggested by Lazar and Tetteroo [28], conservativeness can be further reduced by increasing the order of the Taylor approximation of the nonlinear system.

In summary, our main contributions are as follows:

- We propose a discrete-time network model for vector-borne diseases. This model builds on the continuous-time fully mixed HV-SIS framework introduced in [10], and extends it by embedding the dynamics in a network structure. For this model, we derive general results on the well-posedness of the dynamics, provide reasonable conditions on the discretization time step, and establish the existence of a disease-free equilibrium (DFE).
- We extend the networked HV-SIS model by incorporating two control actions, namely restrictions on human mobility and vector control. At this stage, the spatial network formulation of the HV-SIS model is crucial, as it enables the design and analysis of targeted intervention policies.

- We apply an advanced NMPC scheme to mitigate epidemic spread over the geographic network. Within this framework, we show that the analytical properties of the dynamics are essential to guarantee closed-loop stability and recursive feasibility of the proposed controller, through a suitable choice of terminal ingredients obtained as solutions of a dual offline optimization problem. To the best of our knowledge, this is the first application of NMPC with rigorous guarantees to a networked human–vector epidemic model.
- We validate the framework through numerical experiments, exploring various scenarios of networked HV-SIS models informed by real-world dengue data. These experiments include both a simple 2-node network setting (emulating tropical versus temperate regions) and a realistic network structure based on mobility data across Italy [29]. Beyond validating our framework, the numerical experiments illustrate how our approach can support public health authorities and decision-makers in preventing and counteracting outbreaks of vector-borne diseases.

The remainder of the paper is structured as follows. Section 2 delineates the mathematical framework of the HV-SIS dynamics along with its principal characteristics. Section 3 details the NMPC controller employed, including its theoretical assurances. The results of the numerical simulations are presented in Section 4. Lastly, Section 5 offers conclusions and outlines directions for future research.

2. Network HV-SIS model

We denote by $\mathbb{R}$, $\mathbb{R}_{\geq 0}$, $\mathbb{R}_{>0}$, $\mathbb{N}_{\geq 0}$, and $\mathbb{N}_{>0}$ the real, nonnegative real, strictly positive real, positive integer, and strictly positive integer numbers, respectively. The all-1, all-0 vectors, and identity matrix are denoted by $\mathbf{1}$, $\mathbf{0}$, and I, respectively, with dimensions omitted when clear from the context. Given a square positive definite matrix $W \succ 0$, we denote $\|x\|_W = \sqrt{x^\top W x}$. A function $\delta : \mathbb{R}_{\geq 0} \to \mathbb{R}_{\geq 0}$ is a $\mathcal{K}$-function, if it is continuous, strictly increasing, and $\delta(0) = 0$; it is a $\mathcal{K}$-function if it is also not bounded above. Notation $z_k^{(i)}$ indicates the value of the ith component of z at time $k \in \mathbb{N}_{\geq 0}$. We omit the explicit dependence from i if it is clear from the context.

2.1. Uncontrolled epidemic model over a network

We consider a network of $n \in \mathbb{N}_{>0}$ nodes, labeled with integers $\mathcal{V} = \{1, \dots, n\}$, where each node represents a location in space (e.g., a country or a region). Each location is inhabited by a population of humans with uniform characteristics. Since the duration of an epidemic outbreak is typically negligible with respect to the life-span of humans, we can neglect human demographic dynamics and assume that the population in each node is constant. Assuming that each location contains a large and homogeneous population, the latter is approximated as a continuum of individuals with total mass equal to 1 [5]. Each location also contains a population of disease vectors. Since vectors' life-span is, on the other hand, typically comparable with the disease propagation [30], their relative quantity[1] varies in time, subject to a birth–death process.

The progression of the epidemic is modeled using a susceptible–infected–susceptible (SIS) dynamic framework, where humans may be either susceptible to the disease or infected, and after recovery, they revert to being susceptible. This assumption is a reasonable approximation for numerous vector-borne diseases, such as dengue fever [31]. Let $p_k^{(i)} \in [0, 1]$ represent the fraction of infected individuals at node i at time $k \in \mathbb{N}_{\geq 0}$ (that is, the fraction of susceptible individuals in node is $1 - p_k^{(i)}$). Similarly, vectors at node i can be carriers or non-carriers of the pathogen. Denote by $y_k^{(i)} \geq 0$ and $z_k^{(i)} \geq 0$ the quantities of non-carrier and carrier vectors, respectively. In vector-borne diseases, transmission typically occurs through cross-species interactions, as illustrated in Fig. 1. For example, humans may contract dengue when bitten by an infected (carrier) mosquito, while susceptible (non-carrier) mosquitoes can become carriers after biting infected individuals [31].

Although vectors typically cannot travel long distances during their life cycles [32], humans can. Consequently, susceptible individuals residing in one location can interact with infectious vectors from other locations and thereby import the disease into their home location. This phenomenon, which is of particular concern given the steady increase in air travel [33], can be represented by a directed weighted network $\mathcal{G} = (\mathcal{V}, \mathcal{E}, W)$, where the weight w_{ij} denotes the fraction of the population in location i that travels to location j, and $(i, j) \in \mathcal{E}$ if and only if $w_{ij} > 0$. The diagonal term w_{ii} represents the fraction of the population that remains in location i. In general, the network $\mathcal{G}$ is directed. Moreover, by construction, the sum of all weights originating from any location i is equal to 1, implying that the matrix W is row-stochastic.

For each location $i \in \mathcal{V}$, the three variables $p_k^{(i)}$, $y_k^{(i)}$, and $z_k^{(i)}$ are governed by the following discrete-time dynamics, with discretization time-step $h > 0$:

$$p_{k+1}^{(i)} = (1 - h\gamma)p_k^{(i)} + h\beta_h(1 - p_k^{(i)}) \sum_{j \in \mathcal{V}} w_{ij} z_k^{(j)} \tag{1a}$$

$$y_{k+1}^{(i)} = (1 - h\mu_i)y_k^{(i)} + h\omega_i - h\beta_{vi} p_k^{(i)} y_k^{(i)} \tag{1b}$$

$$z_{k+1}^{(i)} = (1 - h\mu_i)z_k^{(i)} + h\beta_{vi} p_k^{(i)} y_k^{(i)}. \tag{1c}$$

[1] The quantity of vectors is normalized so that the rate of interactions between humans and vectors is proportional to such a quantity. The proportionality constant has no effect on the dynamics, since we will then introduce a parameter that accounts for the contagion rate, which will be rescaled according to this normalization factor and in application scenarios will be tuned against real-world data on the basic reproduction number of the disease under consideration.

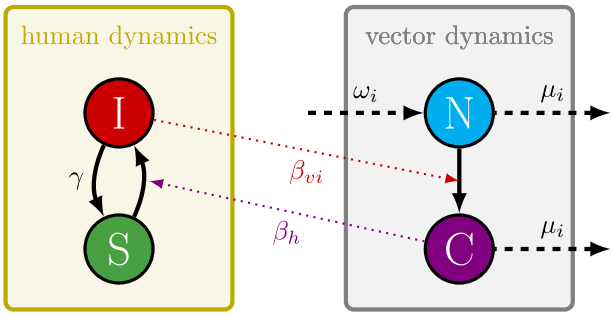


Fig. 1. Schematic of the human-vector epidemic model.

In particular, in (1a), the linear term accounts for recovery, whereby a fraction $\gamma > 0$ is the recovery rate, and thus a fraction γh of infected individuals recovers at each time step, becoming again susceptible to the disease. The nonlinear term in (1a) accounts for local and imported human contagion. The parameter $\beta_h > 0$ captures the human contagion rate. For vectors, instead, the dynamics in (1b) and (1c) is characterized by the vital dynamics, whereby $\mu_i \in [0, 1]$ is the vector death rate (being the inverse of their life-span), so a fraction $h\mu_i$ of vectors die each time-step, and ω_i is the birth rate, so $h\omega_i$ vectors are born in location i at each time-step (which are always non-carriers). We observe that the death rate is independent of the pathogen, since vectors are only carriers and not infected with the disease, so their life-span is not affected by it. Finally, the nonlinear term in (1b) and (1c) accounts for the local transmission from infected humans to vectors, which become carriers. Unlike humans, we have assumed that vectors can have different vital and contagion parameters, since different locations can be inhabited by different species of the vector, with different vital characteristics and susceptibility to become carriers of the pathogen.

For each sampling time k, the $3n$-dimensional vector that gathers all the variables of the system $x = \left[p^{(1)}, \dots, p^{(n)}, y^{(1)}, \dots, y^{(n)}, z^{(1)}, \dots, z^{(n)}\right]^\top$ is the state vector of the networked HV-SIS model. We now observe that, under the following assumption, we can establish some general results on the model.

Assumption 1. Let $h \leq \min_{i\in\mathcal{V}} \left\{ \frac{1}{\gamma}, \frac{\mu_i}{\beta_h \omega_i}, \frac{1}{\mu_i + \beta_{vi}} \right\}$.

Theorem 1. *The discrete-time network HV-SIS model in (1) under Assumption 1 has the following properties:*

(i) The domain $\mathcal{D} := \{x \in \mathbb{R}^{3n} : p^{(i)}, y^{(i)}, z^{(i)} \geq 0, p^{(i)} \leq 1, y^{(i)} + z^{(i)} \leq \frac{\omega_i}{\mu_i}, i \in \mathcal{V}\}$ is positively invariant;

(ii) There exists a unique DFE x_s, with $p_s^{(i)} = z_s^{(i)} = 0$ and $y_s^{(i)} = \frac{\omega_i}{\mu_i}$, for all $i \in \mathcal{V}$; and

(iii) If the trajectory with initial conditions $p_0^{(i)} = 1$, $y_0^{(i)} = 0$, and $z_0^{(i)} = \frac{\omega_i}{\mu_i}$ for all $i \in \mathcal{V}$ converges to the DFE, then all trajectories with initial conditions in $\mathcal{D}$ converge to the DFE.

Proof. (i) Assume that $x_k \in \mathcal{D}$. Then, from (1a), we bound $p_{k+1}^{(i)} \geq (1 - h\gamma)p_k^{(i)} \geq 0$ and $p_{k+1}^{(i)} \leq p_k^{(i)} + (1 - p_k^{(i)})h\beta_h \sum_j w_{ij} \frac{\omega_j}{\mu_j} \leq 1$, from the first and second inequalities in Assumption 1. From (1b) and (1c), we observe that $y_{k+1}^{(i)} \geq (1 - h(\mu_i + \beta_{vi}))y_k^{(i)} \geq 0$ and $z_{k+1}^{(i)} \geq (1 - h\mu_i)z_k^{(i)} \geq 0$, from the third inequality in Assumption 1. Finally, we define $e_{k+1}^{(i)} = \frac{\omega_i}{\mu_i} - y_{k+1}^{(i)} - z_{k+1}^{(i)}$. Since $x_k \in \mathcal{D}$, then $e_k^{(i)} \geq 0$, and we are left to prove that $e_{k+1}^{(i)} \geq 0$. From (1b) and (1c), we obtain $e_{k+1}^{(i)} = (1 - h\mu_i)e_k^{(i)} \geq 0$ due to the third inequality in Assumption 1, which yields the claim.

(ii) Observe that at the DFE (i.e., an equilibrium in which $p_s = z_s = 0$), from (1b), it necessarily holds $y_s = \frac{\omega_i}{\mu_i}$, yielding the claim.

(iii) Operate a change of variables, where we introduce an auxiliary $3n$-dimensional system formed by $p_k^{(i)}$, $z_k^{(i)}$, and $v_k^{(i)} = y_k^{(i)} + z_k^{(i)}$, for all $i \in \mathcal{V}$. By computing the Jacobian matrix of such a system at the generic point of $\mathcal{D}$, we observe that this matrix is Metzler, since all its off-diagonal entries are non-negative. Hence, the dynamical system is monotone [34]. This implies an ordering between the trajectories: given two trajectories with $p_0^{(i)} \geq \tilde{p}_0^{(i)}$, $z_0^{(i)} \geq \tilde{z}_0^{(i)}$, and $v_0^{(i)} \geq \tilde{v}_0^{(i)}$, for all $i \in \mathcal{V}$, then it holds $p_k^{(i)} \geq \tilde{p}_k^{(i)}$, $z_k^{(i)} \geq \tilde{z}_k^{(i)}$, and $v_k^{(i)} \geq \tilde{v}_k^{(i)}$, for all $k \geq 0$ [34]. Hence, if the trajectory with maximal initial conditions $p_0^{(i)} = 1$, and $z_0^{(i)} = v_0^{(i)} = \frac{\omega_i}{\mu_i}$ for all $i \in \mathcal{V}$ (and so $y_0^{(i)} = 0$) converges to the unique DFE, necessarily all other trajectories are upper-bounded by it, and thus converge to the DFE. □

Remark 1. Assumption 1 imposes an upper bound on the discretization time-step h to ensure well-posedness of the dynamics (Theorem 1). In particular, the discretization time-step must be smaller than the characteristic time scales of the system (e.g., the vector life span and the transmissibility period of the disease). This requirement does not limit the generality of the approach, since the control designer can freely select h and, for vector-borne diseases, the characteristic time scales are typically on the order of days or weeks. Consequently, it is computationally feasible to adopt a sufficiently small time-step.

Table 1
Models variables and parameters.

$p_k^{(i)} \in [0,1]$	fraction of infected individuals at node i
$y_k^{(i)} \geq 0$	quantity of non-carrier vectors at node i
$z_k^{(i)} \geq 0$	quantity of carrier vectors at node i
$\beta_h > 0$	human infection rate
$\beta_{vi} > 0$	vector infection rate at node i
$\gamma > 0$	(human) recovery rate
$\omega_i > 0$	vector birth rate at node i
$\mu_i > 0$	vector death rate at node i
$\eta_k^{(ij)} \in [0, w_{ij}]$	mobility reduction from i to j at time k
$\nu_k^{(i)} \in [0, \bar{\nu}_i]$	vector control at node i at time k
$h > 0$	discretization time-step

2.2. Controlled model and problem statement

In this paper, we incorporate two distinct actions in the model that can be enacted to control vector-borne diseases on the human and vector dynamics, respectively.

Human mobility restrictions entail the reduction of human mobility across the network, for example by forbidding travel to regions where the disease is endemic. Here, we assume that such mobility restrictions can be implemented at different continuous levels, ranging from a complete ban, to allowing only essential travel, to no restrictions at all. Hence, for each location $i \in \mathcal{V}$ and time step $k \in \mathbb{N}_{\geq 0}$, we model mobility restrictions by defining a set of $n-1$ control inputs, one associated with each other node, such that mobility from i to j ($i \neq j$) at time k is reduced by $\eta_k^{(ij)} \in [0, w_{ij}]$.[2] In other words, as an effect of the mobility restrictions enacted at time k, human mobility from node i to node j decreases from its baseline value w_{ij} to $w_{ij} - \eta_k^{(ij)}$. Clearly if $w_{ij} = 0$, then the corresponding control input $\eta_k^{(ij)} = 0$ for all $k \in \mathbb{N}_{\geq 0}$, which implies that the number of actual control inputs of the system is equal to the number of edges in the network.

Vector control, instead, consists of reducing the vector population (e.g., by means of insecticides or integrated pest management; see, e.g., {citetWilson2020). We assume that the control designer can decide how much effort to allocate to vector control at each location. Accordingly, for each $i \in \mathcal{V}$ and time step $k \in \mathbb{N}_{\geq 0}$, we model vector control by defining a control input $\nu_k^{(i)} \in [0, \bar{\nu}_i]$ that increases the vector death rate, where $\bar{\nu}_i$ denotes the maximum feasible increase in the vector death rate. In practice, $1/\bar{\nu}_i$ represents the minimum time required to eliminate the maximum achievable fraction of vectors within a single time step. Hence, the incorporation of these two control actions yields the following system, to which we shall refer as the controlled networked HV-SIS model:

$$p_{k+1}^{(i)} = (1 - h\gamma)p_k^{(i)} + h\beta_h(1 - p_k^{(i)}) \sum_{j \in \mathcal{V}} (w_{ij} - \eta_k^{(ij)}) z_k^{(j)} \tag{2a}$$

$$y_{k+1}^{(i)} = (1 - h(\mu_i + \nu_k^{(i)}))y_k^{(i)} + h\omega_i - h\beta_{vi} p_k^{(i)} y_k^{(i)} \tag{2b}$$

$$z_{k+1}^{(i)} = (1 - h(\mu_i + \nu_k^{(i)}))z_k^{(i)} + h\beta_{vi} p_k^{(i)} y_k^{(i)}. \tag{2c}$$

We gather all the control inputs for all $i \in \mathcal{V}$ in a vector $u_k \in \mathbb{R}_{\geq 0}^{n^2}$.

Remark 2. To guarantee that (i) of Theorem 1 holds for the controlled networked HV-SIS model, we need a slightly more restrictive Assumption 1, enforcing $h < \frac{1}{\mu_i + \bar{\nu}_i + \beta_{vi}}$.

Remark 3. The actual number of non-zero control inputs is smaller than n^2, as it depends on the sparsity of the network, as observed when human mobility restrictions are introduced. In practical applications, one can reduce the dimensionality of the control problem by introducing a threshold and approximating the mobility network by removing all edges with weights below this threshold.

All variables and parameters of the model are summarized in Table 1. Next, we introduce an NMPC approach to design an effective control strategy that combines these two types of intervention.

3. NMPC with stability guarantees

Consider the epidemic model described in (2) in its compact and general discrete-time nonlinear formulation

$$x_{k+1} = f(x_k, u_k), \quad k \in \mathbb{N}_{\geq 0} \tag{3}$$

where $x_k = [p_k, y_k, z_k]^\top \in \mathcal{X} \subseteq [0, \infty)^{3n}$ and $u_k = [\eta_k, \nu_k] \in \mathcal{U} \subseteq [0, \infty)^{n^2}$ are the state and the input, respectively, at time $k \in \mathbb{N}_{\geq 0}$. In the following, we assume that the system state is measured[3] at each time instant $k \in \mathbb{N}_{\geq 0}$. Any equilibrium couple of (3) is denoted

[2] For notational convenience, we denote by $\eta^{(j)}$ the mobility reduction from node i to node j whenever this is clear from the context.

[3] If this is not feasible, this assumption can be relaxed by estimating the state via an observer, or by employing an input–output model in place of the state equations.

as (x_s, u_s), such that $x_s = Ax_s + Bu_s$. Additionally, both the state and the input are constrained within two, closed, and compact polytopic regions $x_k \in \mathcal{X} \doteq \{x \in \mathbb{R}^{n_x} : H_x x_k \leq \mathbf{1},\ \forall k\}$ and $u_k \in \mathcal{U} \doteq \{u \in \mathbb{R}^{n_x} : H_u u_k \leq \mathbf{1},\ \forall k\}$, whose interiors are non-empty and $\mathcal{U}$ contain the origin in its interior.

Remark 4. Inspection of (2) shows that the controlled model is continuously differentiable two times. This regularity property will play a crucial role in the development of the stabilizing MPC scheme.

Our control task is to stabilize with an optimal control policy the controlled HV-SIS dynamics in (2) towards an equilibrium (x_s, u_s). To this aim, consider the following MPC cost function:

$$V_N(x, \mathbf{u}) = \sum_{\imath=0}^{N-1} \ell(x_\imath, u_\imath) + V_f(x_N), \tag{4}$$

where $\mathbf{u} = (u_0, u_1, \dots, u_{N-1})$ and N is the prediction horizon. The cost $V_N(x, \mathbf{u})$ is associated with the following NMPC problem, denoted by $\mathcal{P}_N(x)$,

$$\begin{aligned} V_N^*(\hat{x}) = \min_{\mathbf{u}}\ & V_N(x, \mathbf{u}) \\ \text{s.t. } & x_0 = \hat{x}, \\ & x_{\imath+1} = f(x_\imath, u_\imath),\ \imath = 1, \dots, N-1, \\ & x_\imath \in \mathcal{X}, \quad u_\imath \in \mathcal{U}, \quad x_N \in \mathcal{X}_f. \end{aligned} \tag{5}$$

Here, for each $\imath \in \mathbb{N}_{\geq 0}$, $x_\imath = \phi(\imath; x, \mathbf{u})$ is the solution to (3) at time $\imath$ if the initial state is x at $\imath = 0$ and the control is $\mathbf{u}$. Moreover, we define with $\mathcal{X}_N$ the feasible region of the optimal control problem.

The stage cost $\ell(\cdot)$ is the standard quadratic one

$$\ell(x, u) \doteq \|x - x_s\|_Q^2 + \|u - u_s\|_R^2, \tag{6}$$

in which $Q, R \succ 0$ are diagonal matrices of suitable dimensions and the final cost $V_f(\cdot)$ is

$$V_f(\cdot) \doteq \|x_N - x_s\|_P^2, \tag{7}$$

where $P \succ 0$ is one of the terminal ingredients to be chosen for ensuring the closed-loop stability. Finally, as usual in the MPC context, the implicit optimal control law $\kappa_N(x^*)$ is given in a receding horizon fashion and, hence, $\kappa_N(x^*) = u_0^*$.

3.1. Stabilizing NMPC design

In the context of NMPC, closed-loop stability and recursive feasibility rely on a suitable choice of the terminal ingredients $V_f(\cdot)$ and $\mathcal{X}_f$. Indeed, according to Rawlings et al. [17], closed-loop stability is ensured if $V_f(\cdot)$ is a local control Lyapunov function in the neighborhood of the equilibrium and $\mathcal{X}_f$ is positively invariant for the controlled system $x_{k+1} = f(x_k, \kappa_N(x^*))$, such that

$$V_f(x_{k+1}) - V_f(x_k) \leq \ell(x, u), \quad \forall x \in \mathcal{X}_f. \tag{8}$$

A common approach in NMPC consists in finding the terminal ingredients by linearizing the system (3) at the equilibrium point (x_s, u_s) [17,24,28]. Hence, the linearized system is

$$x_{k+1} = Ax_k + Bu_k, \tag{9}$$

where $A = \partial f(x_s, u_s)/\partial x$ and $B = \partial f(x_s, u_s)/\partial u$. As standard in the MPC literature, $V_f(\cdot)$ is a quadratic function such that there exists a symmetric $P \succ 0$ and an associated local linear controller $\kappa_f = u_s + K(x - x_s)$. The terminal set $\mathcal{X}_f \subseteq \mathcal{X}$ is any of the sublevel sets of $V_f(\cdot)$, such that, $\forall \varepsilon > 0$, $\mathcal{X}_f \doteq \{x : V_f(x - x_s) \leq \varepsilon\}$ is positively invariant. For convenience, we denote $A_K \doteq A + BK$, $\tilde{x} \doteq x - x_s$, and $\tilde{u} \doteq u - u_s$.

Remark 5. From Theorem 1, we note that the system (2) is bounded within its domain. Since the linearized system (9) cannot diverge in finite-time, the approximation error $r(x) \doteq f(x, u_s + K\tilde{x}) - x_s - A_K\tilde{x}$ is necessarily locally bounded in the region $\mathcal{X}_N \times \mathcal{U}$.

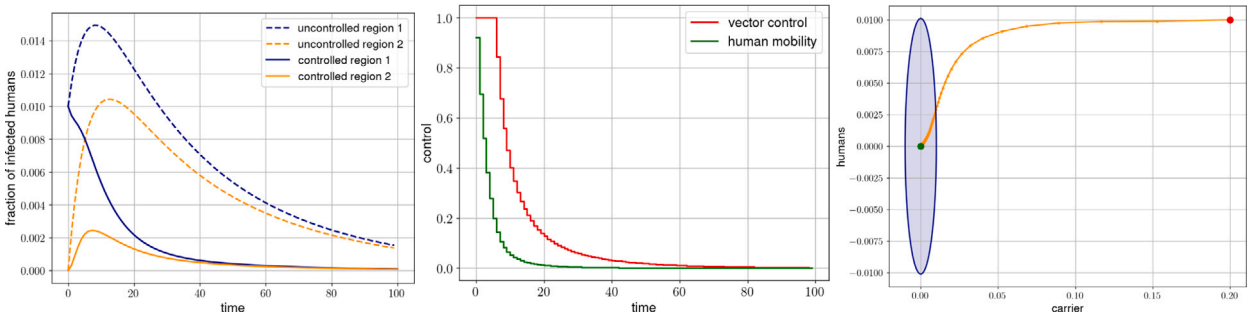
Given the nonlinear system (3) and its linearized counterpart (9), for any $\tau \in (0, 1)$, condition (8) is satisfied [28] if it holds

$$A_K^\top P A_K - (1 - \tau)P + Q + K^\top R K \preceq 0, \tag{10}$$

$$\mathcal{R}(x) \doteq r(x)^\top P r(x) + 2\tilde{x}^\top A_K^\top P r(x) - \tau \tilde{x}^T P \tilde{x} \leq 0, \tag{11}$$

for all $x \in \mathcal{X}_f$. If P can be chosen by solving the LMI in (10), X_f requires a proper tuning of ε ensuring that $\max_{x \in \mathcal{X}_f} \mathcal{R}(x) \leq 0$ [17,35]. Clearly, $\mathcal{X}_f$ can be chosen as the maximal admissible invariant set, satisfying $\mathcal{X}_f \subseteq \mathcal{X}$ and $K\mathcal{X}_f \subseteq \mathcal{U}$.

Thus, we follow the procedure depicted in [28], which allows us to simultaneously find a suitable final control gain K, its associated solution P, and ε maximizing the volume of the terminal ellipsoid. Define $O = P^{-1}$, $Z = A_K O + B_K O$, $Y = KP^{-1}$, and $\bar{\varepsilon} = 1/\varepsilon$. Using Schur's complement, inequality (10) can be written in terms of LMIs.



(a) Fraction of infected nodes (b) Normalized control policy for region 0 (c) Trajectory in region 0

Fig. 2. Simulations for the two-node scenario. In (a), we compare the fraction of infected humans in the uncontrolled (dashed) and controlled (solid) scenarios. In (b), we depict the NMPC control policy for the first node. In (c), we report the trajectory of the controlled dynamics on the carrier–infected plane. The initial conditions and final state are in red and green, respectively, for the first node. The blue ellipse is the terminal set computed through LMI. (For interpretation of the references to color in this figure legend, the reader is referred to the web version of this article.)

To ensure $X_f \subseteq \mathcal{X}$ and $K\mathcal{X}_f \subseteq \mathcal{U}$, the following constraints are imposed during the search of terminal ingredients. Denote by $H_x^{(p)}$ the pth row of H_x and $H_u^{(p)}$ the pth row of H_u. Thus, the LMI

$$\frac{1}{\bar{\varepsilon}} H_x^{(p)\top} O H_x^{(p)} \leq 1 \tag{12}$$

ensures that $X_f \subseteq \mathcal{X}$. In a similar fashion, the LMI

$$\begin{bmatrix} \bar{\varepsilon} & H_u^{(p)\top} Y \\ (H_u^{(p)\top} Y)^\top & O \end{bmatrix} \succeq 0 \tag{13}$$

ensures that $X_f \subseteq K\mathcal{X}$. Thus, the terminal ingredients of the proposed NMPC algorithm are found by solving the following optimization problem:

$$\begin{aligned} P_\varepsilon \quad : \quad & \min_{P,Y,\bar{\varepsilon}} (-\log(\det(O)) + \bar{\varepsilon}) \\ \text{s.t.} \quad & \begin{bmatrix} (1-\tau)O & Z^\top & O & Y^\top \\ Z & O & 0 & 0 \\ O & 0 & \bar{\varepsilon} Q^{-1} & 0 \\ Y & 0 & 0 & \bar{\varepsilon} R^{-1} \end{bmatrix} \geq 0, \\ & \bar{\varepsilon} > 0, \quad O \succ 0, \quad (12), \quad (13). \end{aligned} \tag{14}$$

Solving P_ε provides the value of P and a first guess of ε to construct the terminal ingredients. Indeed, to ensure that the nonlinear inequality (11) holds, it is necessary to check that $\max_{x \in \mathcal{X}_f} \mathcal{R}(x) \geq 0$ using a nonlinear optimization problem. If the condition is not met, ε must be tuned in a suitable way (e.g., using a bisection method) until (11) holds.

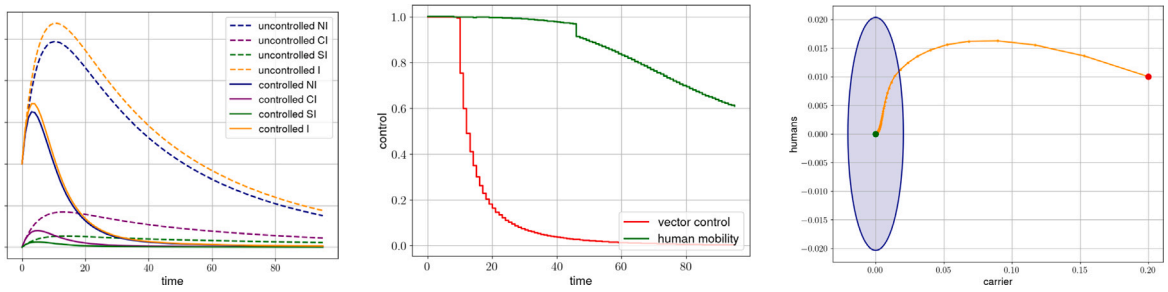
Remark 6. A simpler MMPC design might have consisted of setting $\mathcal{X}_f = \{x_s\}$ and $V_f(\cdot) = 0$ while assuming that there exists a $\mathcal{K}_\infty$ function $\alpha(\cdot)$ such that $V_N^*(\hat{x}) \leq \alpha(|x|)$, $\forall x \in \mathcal{X}_N$. Although the terminal equality constraint design is much simpler than the one proposed in this paper, the price to pay is a sensible reduction of the controller domain of attraction.

4. Numerical simulations

We validate our framework using realistic case studies inspired by dengue outbreaks. Initially, we examine a two-node network representative of a tropical location where dengue is endemic and *Aedes aegypti* mosquitoes are present, along with a temperate location devoid of the disease and its mosquito vectors. Our aim is to underscore the impact of control measures on the proportion of infected individuals at equilibrium. Subsequently, we expand our analysis to a more comprehensive and realistic scenario involving a network of Italian macro-areas, utilizing mobility data derived from census information [29].

4.1. Two-node scenario

In the initial simulation study, we examine a two-node scenario. Node 1 represents a tropical location where dengue is endemic, infested by *Aedes aegypti*; node 2 represents a temperate region where dengue is not endemic and *Aedes albopictus* are prevalent. Although the latter can still transmit dengue, it does so with a lower probability, as indicated in [36]. Consequently, we assume



(a) Fraction of infected nodes (b) Control policy in Northern Italy (c) Trajectory in Northern Italy

Fig. 3. Simulations for the macro-region scenario with two starting contagion areas (Northern Italy and Islands). In (a), the fraction of infected humans in the uncontrolled (dashed) and controlled (solid) scenarios. In (b), the NMPC control policy in Northern Italy. In (c), the trajectory of the controlled dynamics on the carrier–infected plane related to Norther Italy. The initial conditions and final state are in red and green, respectively. The blue ellipse is the terminal set computed through LMI. (For interpretation of the references to color in this figure legend, the reader is referred to the web version of this article.)

heterogeneity in vector infection rates. Referencing [30,36,37], and adjusting the parameters with a time step of $h = 1$ day, we define the human infection rate as $\beta_h = 0.0286$, vector infection rates as $\beta_{v1} = 0.0714$ and $\beta_{v2} = \frac{1}{2}\beta_{v1} = 0.0357$, human recovery rate as $\gamma = 0.143$, and vector birth and death rates as $\omega_1 = \omega_2 = \mu_1 = \mu_2 = 0.0357$, measured in day^{-1}. This choice guarantees that Assumption 1 is satisfied.

The system is initialized with conditions $x_1 = (0.01, 0, 0.2)$ and $x_2 = (0, 0, 0)$. The target equilibrium (x_s, u_s) is the DFE calculated as per Theorem 1. For stage cost $\ell(\cdot)$, aligning with our primary goal of minimizing epidemic prevalence, we configure Q as block-diagonal with larger entries for the block associated with human infections. In particular, we set weights 10^3 for human infection entries, 10^{-8} for non-carrier vectors, and 1 for carriers. This choice is arbitrary, but it guarantees that the remaining entries are negligible with respect to human infections, thereby keeping the matrix Q positive definite, which is essential for the control design. For robustness, we conducted additional simulations in which we varied the values of the entries (while preserving their relative ordering) and observed no quantitative changes in the outcomes.

For the matrix R, unless otherwise stated, we set it equal to the identity matrix. This configuration of R ensures equal marginal penalties for both control actions, namely human mobility restrictions and vector death rate, thus maintaining neutrality in preferences. Clearly, increasing the entries of the block associated with one type of control action relative to the other would introduce a bias in the preferred control action toward the less penalized one. The terminal set, as a sub-level of $V_f(\cdot)$ is uniquely determined by $\varepsilon = 2.06236e{-}4$. Note that $\max_{x \in \mathcal{X}_f} \mathcal{R}(x) \geq 0$ is satisfied without any additional shrinkage of ε. Finally, we set $N = 110$. This high value for the prediction horizon is comparable with realistic epidemic prediction horizons of a few months. To face NMPC computational costs, future work could optimize intervention policy by adopting a more realistic decision cadence: governments typically do not update control measures daily but reassess them in weekly or bi-weekly cycles, as occurred during COVID-19 [38]. This can be formalized by introducing discrete intervention times at which a new control is computed, while the dynamics evolve in between under a piecewise-constant control. Other alternatives may consist of widening the domain of attraction of the controller by implementing an NMPC for reference tracking [24].

Simulation results are reported in Fig. 2. In particular, in Fig. 2(a), we compare the uncontrolled dynamics (dashed curves) with the controlled one (solid curves). The resulting optimal control actions of the NMPC are shown in Fig. 2(b). For clarity of presentation, the control policy is represented here with a normalization with respect to the maximum admissible control action. Interestingly, the optimal intervention policy seems to involve both types of actions. Initially, both control actions are enacted, with mobility restrictions gradually uplifted while the epidemic reaches its peak. Importantly, we observe that the number of infected individuals at peak is halved compared to the uncontrolled scenario (Fig. 2(a)). Vector control policies, instead, start to increase only after the peak in human contagion has passed, and the number of mosquitoes is sufficiently small to avoid surges in the number of carriers. The projection of the terminal set $\mathcal{X}_f$ — on the human/carrier plane — is represented in Fig. 2(c) by the blue ellipse. There, we also report the trajectory for the "tropical" node. The final state reached, as expected, is the DFE (green dot).

4.2. Italian network

In the second simulation study, we consider a realistic scenario of a 4-node network corresponding to Italian macro-areas, i.e. Northern Italy, Central Italy, Southern Italy, and Islands. The network of human mobility W is estimated from real-world census data on daily mobility across different provinces [29] and then aggregated and normalized to account for the different populations in the macro-areas. The simulation uses the same parameter settings as in the two-node scenario, with an homogeneous vector infection rate $\beta_v = 0.0714$.

Since the weight matrix is strongly diagonally dominant, we let the contagion start from two regions (Northern Italy and Island), i.e. the system starts from the following initial conditions: $x_1 = x_4 = (0.01, 0, 0.2)$ and $x_2 = x_3 = (0, 0, 0)$. The general setting of the

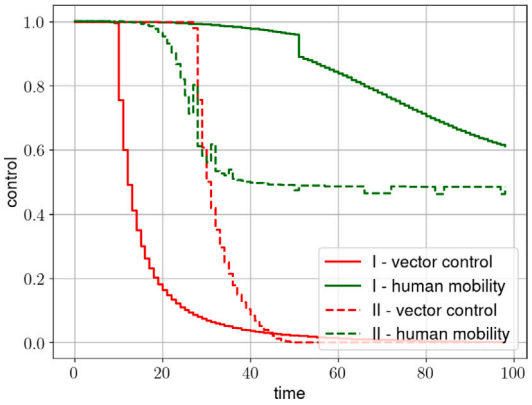


Fig. 4. Comparison of control policies as function of cost matrix R in Northern Italy. Case I (solid): higher cost for vector control; Case II (dashed): higher cost for action on human mobility.

problem remains unchanged. The terminal set, as a sub-level of $V_f(\cdot)$ is uniquely determined, using LMI, by $\varepsilon = 4.176691e{-}4$. In this case, also $\max_{x\in\mathcal{X}_f} \mathcal{R}(x) \geq 0$ is satisfied without any additional shrinkage of ε. We consider a prediction horizon of $N = 150$, which does not significantly affect the model performance. Notably, the results were obtained several orders of magnitude faster than the system time-step (approximately 2 min for the entire prediction horizon on a standard laptop), making the proposed approach feasible for real-time implementations, even for larger networks.

The results, which further corroborate the validity of the proposed control strategy in this more general setting, are reported in Fig. 3. Fig. 3(a) compares the fraction of infected humans under uncontrolled (dashed) versus controlled (solid) dynamics across all macro-areas, showing a clear, non-negligible improvement with control. Fig. 3(b) restricts the analysis to Norther Italy region and shows the control inputs, normalized by their maximum admissible levels under the assumption that the two control actions have equal cost. Initially, both controls are active until the infection peaks have passed. After that point, vector-control policies drop rapidly, while stringent restrictions on human mobility remain in place. As expected, Fig. 3(c) shows that the system trajectories evolve and ultimately converge to the DFE (green dot). Also in this case the analysis is restricted to Northern Italy region for representative reasons.

Finally, Fig. 4 illustrates the dependence of the NMPC policy on the cost matrix R. In particular, we compare Case I, in which vector control is more expensive (solid curve), with Case II, in which human-mobility control carries the higher cost (dashed curve). The two cases are constructed by setting the diagonal entries of R associated with human mobility to 10^{-3} and those associated with vector control to 1 for Case I, and by reversing this choice for Case II. As expected, the control policy is sensitive to the relative costs, with the less expensive intervention generally being favored. Nonetheless, even under substantial disparities in the cost weights, the optimal control strategy involves a non-trivial combination of both interventions.

5. Conclusion

In this paper, we develop a nonlinear Model Predictive Control (NMPC) scheme for controlling a vector-borne epidemic by implementing human mobility restrictions and reducing the carrier population. The proposed NMPC framework provides closed-loop stability guarantees, achieved through an appropriate design of the terminal ingredients of the controller. In particular, the terminal cost and terminal region are computed by linearizing the system around the reference equilibrium, and subsequently solving two sequential offline optimization problems to determine the terminal feedback gain and the size of the terminal region. The effectiveness of the framework is demonstrated through realistic dengue case studies: (i) a two-node network as in [10], and (ii) a four-node network representing Italian macro-areas, using mobility data from ISTAT [29].

The promising results presented in this paper suggest several directions for future research. First, the proposed approach can be extended to more complex dynamics of vector-borne epidemic spreading by incorporating factors such as natural immunity, heterogeneous transmissibility levels, and seasonal variations in model parameters. Second, we have assumed that control inputs are continuous-valued functions. In many real-world scenarios, however, only a finite set of interventions may be available (e.g., a limited number of mobility restriction levels). While our results remain useful for providing insights into the design of optimal intervention policies, future work should investigate control strategies with discrete-valued inputs. Third, the proposed MPC scheme is fully centralized. Although this is consistent with the structure of many healthcare systems, it may be suboptimal, as it can reduce robustness to controller malfunction and increase computational complexity. Alternative hierarchical and partially decentralized MPC architectures could be explored, potentially incorporating a lower-level cooperative MPC framework to manage epidemic spread within smaller regional areas. Fourth, other advanced MPC schemes, such as robust MPC (when the system state is not fully measurable), economic MPC, or MPC for reference tracking, could be employed. The latter option, in particular, may be beneficial for enlarging the controller's domain of attraction, thereby allowing a shorter prediction horizon while still ensuring recursive feasibility of the optimal control problem. Consequently, the computational complexity of the optimal control problem could be reduced.

CRediT authorship contribution statement

Roberta Raineri: Writing – review & editing, Writing – original draft, Visualization, Validation, Software, Formal analysis, Data curation, Conceptualization. **Michele Pagone:** Writing – review & editing, Writing – original draft, Supervision, Methodology, Investigation, Formal analysis, Conceptualization. **Lorenzo Zino:** Writing – review & editing, Writing – original draft, Validation, Supervision, Methodology, Investigation, Formal analysis, Data curation, Conceptualization. **Alessandro Rizzo:** Writing – review & editing, Supervision, Resources, Project administration, Funding acquisition, Conceptualization.

Declaration of competing interest

The authors declare the following financial interests/personal relationships which may be considered as potential competing interests: Roberta Raineri , Lorenzo Zino reports financial support was provided by Government of Italy. If there are other authors, they declare that they have no known competing financial interests or personal relationships that could have appeared to influence the work reported in this paper.

Data availability

No data was used for the research described in the article.

References

[1] C. Nowzari, V.M. Preciado, G.J. Pappas, Analysis and control of epidemics: a survey of spreading processes on complex networks, IEEE Control Syst. Mag. 36 (1) (2016) 26–46.
[2] L. Zino, M. Cao, Analysis, prediction, and control of epidemics: A survey from scalar to dynamic network models, IEEE Circ. Syst. Mag. 21 (4) (2021) 4–23.
[3] T. Alamo, D. G. Reina, P. Millán Gata, V.M. Preciado, G. Giordano, Data-driven methods for present and future pandemics: Monitoring, modelling and managing, Annu. Rev. Control. 52 (2021) 448–464.
[4] L. Calogero, M. Pagone, L. Zino, A. Rizzo, An economic nonlinear model predictive control approach for mitigating epidemic spreading on networks, in: Proc. 64st IEEE CDC, 2025.
[5] W. Mei, S. Mohagheghi, S. Zampieri, F. Bullo, On the dynamics of deterministic epidemic propagation over networks, Annu. Rev. Control. 44 (2017) 116–128.
[6] P.E. Paré, C.L. Beck, T. Başar, Modeling, estimation, and analysis of epidemics over networks: An overview, Annu. Rev. Control 50 (2020) 345–360.
[7] World Health Organization, Vector-borne diseases, 2025, https://www.who.int/news-room/fact-sheets/detail/vector-borne-diseases.
[8] M. Aguiar, et al., Mathematical models for dengue fever epidemiology: A 10-year systematic review, Phys. Life Rev. 40 (2022) 65–92.
[9] S.T. Ogunlade, M.T. Meehan, A.I. Adekunle, E.S. McBryde, A systematic review of mathematical models of dengue transmission and vector control: 2010–2020, Viruses 15 (1) (2023) 254.
[10] L. Zino, A. Casu, A. Rizzo, A human-vector susceptible–Infected–susceptible model for analyzing and controlling the spread of vector-Borne diseases, in: Proc. 23rd Eur. Control Conf., 2025, pp. 1219–1224.
[11] A. Padder, S. Qureshi, A.E. Matouk, K. Dehingia, Dynamical analysis of a vector-borne disease model with control function strategies, Discov. Appl. Sci. 7 (9) (2025).
[12] Manisha, A. Kumar, Modeling and optimal management of control policies for vector-Borne diseases: A study of cost-effectiveness and policy impact, Optimal Control Appl. Methods 46 (6) (2025) 2882–2915.
[13] K. Blayneh, Y. Cao, H.-D. Kwon, Optimal control of vector-borne diseases: Treatment and prevention, Discret. Contin. Dyn. Syst. Ser. B 11 (3) (2009) 587–611.
[14] S. Boulaaras, M. Yavuz, Y. Alrashedi, S. Bahramand, R. Jan, Modeling the co-dynamics of vector-borne infections with the application of optimal control theory, Discret. Contin. Dyn. Syst. Ser. B 18 (5) (2025) 1331–1352.
[15] A. Ferramosca, D. Limon, I. Alvarado, E.F. Camacho, Cooperative distributed MPC for tracking, Automatica 49 (2013) 906–914.
[16] F. Parino, L. Zino, G.C. Calafiore, A. Rizzo, A model predictive control approach to optimally devise a two-dose vaccination rollout: A case study on COVID-19 in Italy, Int. J. Robust Nonlin. Control. 33 (9) (2021) 4808–4823.
[17] J. Rawlings, D. Mayne, M. Diehl, Model Predictive Control: Theory, Computation, and Design, Nob Hill Publishing, 2017.
[18] J. Köhler, L. Schwenkel, A. Koch, J. Berberich, P. Pauli, F. Allgöwer, Robust and optimal predictive control of the COVID-19 outbreak, Annu. Rev. Control. 51 (2021) 525–539.
[19] T. Péni, G. Szederkényi, Convex output feedback model predictive control for mitigation of COVID-19 pandemic, Annu. Rev. Control. 52 (2021) 543–553.
[20] M.M. Morato, S.B. Bastos, D.O. Cajueiro, J.E. Normey-Rico, An optimal predictive control strategy for COVID-19 (SARS-CoV-2) social distancing policies in Brazil, Annu. Rev. Control. 50 (2020) 417–431.
[21] J. Sereno, A. D'Jorge, A. Ferramosca, E. Hernandez-Vargas, A. González, Switched NMPC for epidemiological and social-economic control objectives in SIR-type systems, Annu. Rev. Control. 56 (2023) 100901.
[22] H. Chen, F. Allgöwer, A quasi-infinite horizon nonlinear model predictive control scheme with guaranteed stability, Automatica 34 (10) (1998) 1205–1217.
[23] Z.-P. Jiang, Y. Wang, Input-to-state stability for discrete-time nonlinear systems, Automatica 37 (6) (2001) 857–869.
[24] D. Limon, A. Ferramosca, I. Alvarado, T. Alamo, Nonlinear MPC for tracking piece-wise constant reference signals, IEEE Trans. Autom. Control 63 (11) (2018) 3735–3750.
[25] M. Pagone, M. Boggio, C. Novara, A. Proskurnikov, G.C. Calafiore, Continuous-time nonlinear model predictive control based on Pontryagin Minimum Principle and penalty functions, Internat. J. Control 98 (4) (2025) 765–781.
[26] Z. Wan, M.V. Kothare, An efficient off-line formulation of robust model predictive control using linear matrix inequalities, Automatica 39 (5) (2003) 837–846.
[27] Z. Wan, M.V. Kothare, Efficient scheduled stabilizing model predictive control for constrained nonlinear systems, Int. J. Robust Nonlin. Control. 13 (3–4) (2003) 331–346.
[28] M. Lazar, M. Tetteroo, Computation of terminal costs and sets for discrete-time nonlinear MPC, in: Proc. 6th IFAC Conf. NMPC, 51, (20) 2018, pp. 141–146.
[29] ISTAT, Istituto Nazionale di Statistica, 2025, https://www.istat.it.

[30] J. Lourenço, M. Recker, Viral and epidemiological determinants of the invasion dynamics of novel dengue genotypes, in: R. Rico-Hesse (Ed.), PLOS Negl. Trop. Dis. 4 (11) (2010) e894.
[31] World Health Organization, Dengue and severe dengue, 2025, https://www.who.int/health-topics/dengue-and-severe-dengue.
[32] M.S. Bogojević, T. Hengl, E. Merdić, Spatiotemporal monitoring of floodwater mosquito dispersal in Osijek, Croatia, J. Am. Mosq. Control Assoc. 23 (2) (2007) 99–108.
[33] A.J. Tatem, Z. Huang, A. Das, Q. Qi, J. Roth, Y. Qiu, Air travel and vector-borne disease movement, Parasitology 139 (14) (2012) 1816–1830.
[34] M.W. Hirsch, Attractors for discrete-time monotone dynamical systems in strongly ordered spaces, in: Geometry and Topology, Springer Berlin Heidelberg, 1985, pp. 141–153.
[35] D. Mayne, An apologia for stabilising terminal conditions in model predictive control, Internat. J. Control 86 (11) (2013) 2090–2095.
[36] C. Fortuna, et al., Assessing the risk of dengue virus local transmission: Study on vector competence of Italian Aedes albopictus, Viruses 16 (2) (2024).
[37] P. Bhatt, S.P. Sabeena, M. Varma, G. Arunkumar, Current understanding of the pathogenesis of dengue virus infection, Curr. Microbiol. 78 (1) (2021) 17–32.
[38] Y. Bo, et al., Effectiveness of non-pharmaceutical interventions on COVID-19 transmission in 190 countries from 23 January to 13 April 2020, Int. J. Infect. Dis. 102 (2021) 247–253.